Journal of Chromatography, 500 (1990) 481–502
Elsevier Science Publishers B.V., Amsterdam — Printed in The Netherlands

CHROM. 22 131

INTRINSIC FLUORESCENCE STUDIES OF THE KINETIC MECHANISM OF UNFOLDING OF α-LACTALBUMIN ON WEAKLY HYDROPHOBIC CHROMATOGRAPHIC SURFACES

PETER OROSZLAN, RIGOBERTO BLANCO, XIAO-MING LU[a], DAVID YARMUSH[a] and BARRY L. KARGER*

Barnett Institute, Northeastern University, Boston, MA 02115 (U.S.A.)

(First received September 22nd, 1989; revised manuscript received November 1st, 1989)

SUMMARY

The kinetic mechanism of unfolding of calcium depleted bovine α-lactalbumin adsorbed on two weakly hydrophobic chromatographic surfaces, methyl- and ethyl-polyether phases bonded to porous silica, with a solution phase of 3 *M* ammonium sulfate at pH 6.3, has been determined using intrinsic fluorescence and liquid chromatography (LC). The adsorbent has been packed into quartz flow cells which are used for both fluorescence measurements and as a microcolumn for LC. The LC measurements revealed two peaks for α-lactalbumin on both phases, the first being folded and the second unfolded. The rate of unfolding was measured to be $1.75 \cdot 10^{-3}$ min^{-1} on the C1-ether and $7.42 \cdot 10^{-3}$ min^{-1} on the C2-ether phase. Fluorescence studies revealed a slow change in emission maximum from *ca.* 330 nm to 350 nm and a 4-fold increase in intensity for the protein adsorbed on the two supports. Variation of fluorescence intensity at a given wavelength revealed biphasic kinetics in which the rate law on the surface was deduced as $F \rightleftharpoons X \rightarrow U$, where F is the folded form, U an unfolded form and X an intermediate. The normalized emission spectra of the three species were calculated and it was found that there was approximately a 20-nm-red shift in the position of the maximum from F to U. The emission maximum for X was close to U on both columns; however, the normalized intensity for X was between F and U. Activation enthalpies and entropies were determined from the temperature dependence of the microscopic rate constants. The formation of the intermediate on the C1-ether phase was entropy driven whereas on the C2-ether phase it was enthalpy driven. Finally, the solution refolding rates of U desorbed from the two supports were found to be identical. The differences observed in the surface kinetics of unfolding on the two supports are related to the hydrophobic differences of the adsorbents.

[a] Present address: Department of Chemical and Biochemical Engineering, Rutgers University, Piscataway, NJ 08855, U.S.A.

0021-9673/90/$03.50

INTRODUCTION

Studies of protein adsorption are important from both fundamental and practical points of view. An understanding of the sorption process will aid in the development of realistic models of the behavior of proteins at interfaces as well as in the understanding of the interaction of proteins with various surfaces, a topic of significance in the development of biocompatible materials[1]. From the separation point of view, it is also important to understand protein adsorption in order to optimize conditions for resolution and to minimize the loss of biological activity or mass of the protein[2].

It is well established that when a protein or polypeptide comes in contact with an adsorbent surface, structural or conformational changes can occur as the species responds to the non-physiological environment[3]. Indeed, chromatography often involves the manipulation of conformation, knowingly or unknowingly, in order to achieve separation. Since significant differences in free energies of adsorption can exist for various conformers, the rational alteration of conformation can provide a powerful approach to selectivity control. Frequently, the effect of various parameters, such as salt, pH, buffer and temperature, on separation (and sample loading capacity) is difficult to predict due to the alteration of protein conformation with a given parameter change. In addition, depending on the rate of structural change, broadened and asymmetrical or multiple peaks may be observed[4]. Furthermore, conformational manipulation should not be so extensive that irreversible alteration in structure and function results[5].

Based on the above discussion, an understanding of protein structural behavior on adsorbent surfaces (and in the mobile phase) is significant. Most studies of protein adsorption to-date have been indirect, *i.e.* the adsorption coefficient or the characteristics of the desorbed protein in solution are measured[6,7]. However, characterization of the protein while in direct contact with the adsorbent surface is required for analysis of what structural changes and rates of change actually take place on the surface. Some attempts at characterization of the adsorbed protein have occurred, *e.g.* antibody binding against epitopes[8], ellipsometry[9], Raman[10], circular dichroism[11] and Fourier-transform infrared spectroscopy[12].

Another approach which appears quite powerful is intrinsic fluorescence spectroscopy, which is known to be an important tool in the study of the kinetics of protein conformational changes in solution[13]. The fluorescence emission signal is sensitive to changes in the microenvironment of the protein fluorophores, especially tryptophan, and useful kinetic information about the unfolding–refolding process can be obtained. Some recent reports also discuss the capability of fluorescence to probe *in situ* the conformation of protein adsorbed to surfaces. Gabel *et al.*[14] first described a fluorometric technique (front-faced) to study proteins bound to the surface of Sephadex. Since then, progress has been made in applying fluorescence spectroscopy to adsorbed proteins, especially with the use of total internal reflectance spectroscopy[15,16].

Direct intrinsic fluorescence has recently been utilized for the study of adsorbed proteins on chromatographic surfaces. In one approach, conformational changes were deduced on the basis of changes in the wavelength of emission maximum[17]. Recently, we have demonstrated that the kinetics of change of proteins on a surface can also be

followed by an examination of the fluorescence of the adsorbed protein[18,19]. This approach can provide significant insight into what is occurring while the protein is in contact with the surface. The purpose of this paper is to define the methodology in detail and to demonstrate the power of the approach in elucidating kinetic processes on the surface, using as example bovine α-lactalbumin (α-LACT) on two weakly hydrophobic adsorbents.

α-LACT is a good protein for study since its solution conformational behavior has already been widely examined by fluorescence[20–23]. In the solution unfolding process at neutral pH, an intermediate state has been observed which bears similarity to the well characterized thermal or acid unfolded states of the protein[23–25]. In addition, hydrophobic interaction chromatographic (HIC) studies of α-LACT on two weakly hydrophobic supports suggested conformational changes on the surface[26,27]. Thus, a study combining fluorescence and HIC for examining the adsorbed behavior of α-LACT is warranted.

MATERIALS AND METHODS

Equipment

The instrumental components are shown in Fig. 1. Fluorescence measurements were made with a SPF-500 spectrofluorometer (SLM-Aminco, Urbana, IL, U.S.A.). A Suprasil quartz spectroscopic flow cell (35 μl, 11 × 2 mm I.D.) was utilized both for the surface fluorescence measurements and as a microchromatographic column. A Series 410 BI0 LC liquid chromatographic pump (Perkin-Elmer, Norwalk, CT, U.S.A.) was attached to the inlet of the packed fluorescence cell and the outlet of the cell was connected to a 1046A fluorescence LC detector (Hewlett-Packard, Palo Alto, CA, U.S.A.) via an empty spectroscopic flow cell. The sample compartment, injector and tubing (PTFE, 0.3 mm I.D. × 1.5 mm O.D.) attached to the column were thermostated to ±0.1°C by an Exacal and FTC Model 350A flow-through cooler system (Neslab, Newington, NH, U.S.A.), controlled by a thermocouple (Omega, Stanford, CT, U.S.A.). The chromatographic and spectroscopic data were processed

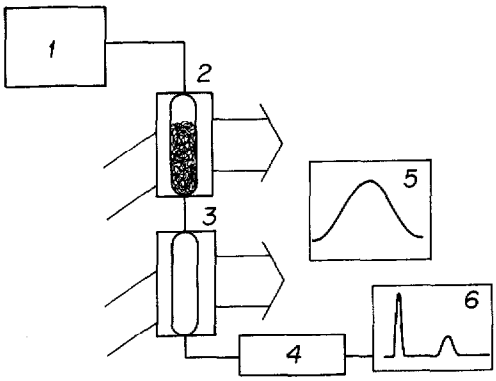

Fig. 1. Instrument block diagram. 1 = HPLC pump; 2 = 35-μl flow cell packed column (cell I); 3 = 35-μl empty flow cell (cell II); 4 = fluorescence chromatographic detector; 5 = emission fluorescence spectrum; 6 = chromatogram. See Experimental for details.

with a data acquisition system (Nelson Analytical, Cupertino, CA, U.S.A.) and Spectrum Processor software (SLM Instruments, Urbana, IL, U.S.A.).

The first fluorescence cell was carefully packed with roughly 25 mg of Vydac silica gel (Separations Group, Hesperia, CA, U.S.A.) bonded with both methyl (C1-ether) and ethyl (C2-ether) polyether phase (particle size 5 μm, pore diameter 300 Å, specific surface area 72 m^2/g) and prepared as described elsewhere[28]. The surface coverages were 6.3 and 4.6 $\mu mol/m^2$, for C1-ether and C2-ether, respectively, as determined by elemental analysis (assuming a stoichiometry of 2 for the binding of the silane to silica). The packing was accomplished slowly by hand to obtain a homogeneous distribution of the support in the column. Slurring packing with organic solvents was not used, in order to avoid entrapment of the solvent in the bonded phase, as well as to prevent cell breakage. Column conditioning was accomplished by injecting 10-μl aliquots of a 5.0-mg/ml protein solution 20 times, followed each time by elution under HIC gradient conditions. In this manner a constant surface for the kinetic studies was achieved as indicated by the reproducibility of the fluorescence kinetics and chromatographic results (see Results and Discussion).

Chemicals

Calcium depleted bovine milk α-LACT was purchased from Sigma (St. Louis, MO, U.S.A.). The purity of the protein was determined by reversed-phase liquid chromatography and size-exclusion chromatography. Only one sharp peak was found in both cases. In addition, the fluorescence emission maximum of the protein in water (pH 7) was found to be identical to that reported in the literature[29]. Therefore, the sample was assumed to be sufficiently pure for chromatographic and fluorescence experiments. HPLC water, ammonium sulfate and ammonium acetate were purchased from J. T. Baker (Phillipsburg, NJ, U.S.A.). Mobile phases were passed through an 0.45-μm filter, degassed by vacuum and sparged with helium before use.

Care was taken to avoid a possible Ca^{2+} uptake of α-LACT from the system. All glassware and cuvettes were carefully washed with 50% nitric acid and rinsed several times with deionized water. Finally, the system was washed with 0.0033 *M* phosphate buffer and rinsed with deionized water.

Procedures

A relatively high voltage was applied to the photomultiplier of the sample cell (900 V) and that of the reference cell (250 V), and a gain ratio of 10:1 was used. The detection limit (signal-to-noise ratio 2) of the protein was 5 μg. Experimentally, a 10-μl injected volume of a 5-mg/ml sample (50 μg) of α-LACT was determined as a convenient amount for the surface fluorescence study. The collected spectra were electronically smoothed in order to minimize random noise. The reproducibility of maximum emission intensity at fixed sampling time for independent injections of the same protein solution on the column was 0.5% coefficient of variation (C.V.; $n = 5$). The absolute intensity measured in different columns at a fixed sampling time was strongly dependent on the total amount of adsorption surface available, as well as, surface scattering effects; however, the normalized spectra (see Results and Discussion) were observed to have the same shape from column to column, *i.e.* the normalized spectra were superimposable over the whole range of wavelengths sampled.

The incubation solvent (see below) transported the sample of 10 μl of the protein (5 mg/ml in 1 *M* (ammonium sulfate) into the flow cell column (cell I). The time of solute travel from the injector (including the sample loop) to the column, at a flow-rate of 0.3 ml/min, was 12 s. Thus, 12 s after injection was defined as the initial surface contact time of the protein, *i.e.* zero time. A 10-min linear gradient from 100% solvent A (3 *M* ammonium sulfate, 0.5 *M* ammonium acetate, pH 6.3) to 100% B (0.5 *M* ammonium acetate, pH 6.3) was used to elute the protein from the flow cell column after a given period of time of contact with the surface. The time from cell I to the second empty cell (II) was determined to be 6 s and to the fluorescence detector to be 34 s at a mobile phase flow-rate of 0.3 ml/min.

RESULTS AND DISCUSSION

Hydrophobic interaction chromatography

The chromatographic behavior of α-LACT under HIC conditions, using the two hydrophobic supports, the C1-ether and the C2-ether bonded phases, has been previously reported[26,27]. In that work, only one peak was found on the C1-ether phase; however, two well-resolved peaks were observed on the more hydrophobic C2-ether phase, suggesting a surface induced unfolding of the protein[4]. The relative amounts of these two peaks on the C2-ether phase were time and temperature dependent; increased incubation time produced a decrease in the area of the first peak and a proportional increase in the area of the second peak. The increase in temperature accelerated the process. It was also found that the second peak, identified as the unfolded protein by on-line second-derivative UV spectroscopy, could rapidly refold in solution, the eluted fraction producing the first peak upon reinjection in the chromatographic system.

Fig. 2A presents the chromatograms obtained in the present study by gradient elution under different protein surface contact times on the C1-ether phase in the packed fluorescence cell, pH 6.3, 4°C. In contrast to the above cited work, two sharp peaks were observed (elution compositions of the mobile phase B of 48% and 77%, respectively), albeit for much longer incubation times, with the ratio of the areas changing as a function of contact time. In order to calculate the kinetic constant of the assumed unfolding process, the area of the first peak, which was presumed to represent the folded form, was determined as a function of time.

The first order plot of ln (area of the first peak) *vs.* time produced a straight line ($r^2 = 0.9957$) with a rate constant equal to $1.75 \cdot 10^{-3}$ min^{-1}. From this result, it can be understood why previously only one peak was observed on the C1-ether phase[26], since the half-life for the unfolding process was in the order of 400 min and the largest time used in those experiments was 60 min.

Similar experiments were performed using the C2-ether phase (see Fig. 2B). Two peaks were again observed, but the second was now broad, in agreement with earlier results[27]. In addition, in comparison to the less hydrophobic C1-ether phase, both peaks exhibited longer retention time (66% and 100% mobile phase B for the first and the second peak, respectively). From the decrease of the area of the first peak with time, the first order rate constant was calculated to be $7.42 \cdot 10^{-3}$ min^{-1} ($r^2 = 0.9962$). There was a more rapid conversion to the second peak on the more hydrophobic stationary phase. The broadening can be explained in part by the required isocratic conditions for elution.

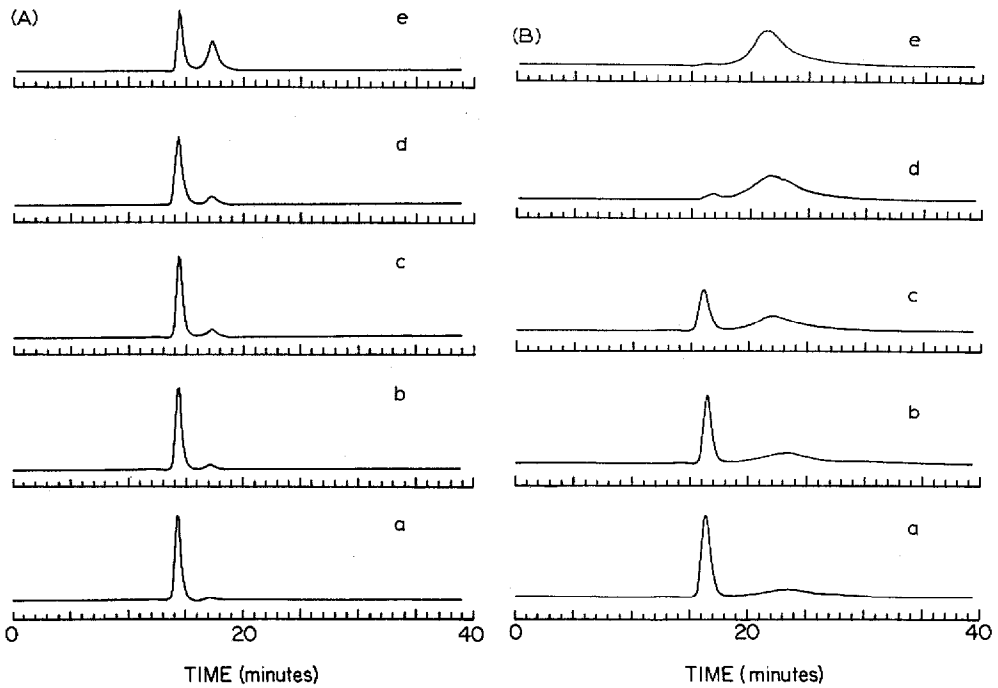

Fig. 2. Gradient elution chromatograms of α-LACT as a function of incubation time. (A) C1-ether phase: (a) 0, (b) 30, (c) 60, (d) 120 and (e) 930 min incubation time. (B) C2-ether phase: (a) 0, (b) 30, (c) 60, (d) 420 and (e) 900 min incubation time. Conditions: 10-min gradient from 100% mobile phase A (3 *M* ammonium sulfate plus 0.5 *M* ammonium acetate, pH 6.3) to 100% B (0.5 *M* ammonium acetate, pH 6.3). Detection wavelength: 350 nm, flow 0.3 ml/min, temperature 4°C.

In order to explore this unfolding process in greater detail, we next examined the *in situ* fluorescence of the species on the surface as a function of time. We first discuss several aspects of the surface fluorescence measurements followed by a detailed examination of the kinetic processes.

Elimination of fluorescence interferences

Two potential interferences in intrinsic fluorescence studies of adsorbed proteins are photodecomposition of the tryptophan residues and light scattering[14]. Exposure of the system to intense UV radiation can produce photodecomposition reactions which may affect the emission signal, introducing spurious intensity changes. Kinetic results could thus be altered since emission intensity as a function of time is measured.

In order to minimize photodecomposition, particularly for slow kinetic changes, a discontinuous method of data collection was followed. The fluorescence intensity was collected by scanning for 10 s from 325 nm to 355 nm at 30, 120, 300 and 600 s after injection and during incubation. This discrete measurement procedure produced two important advantages: first, the fluorescence intensity was collected as a function of time without continuous exposure of the protein to high intensity UV radiation. Secondly, complete emission spectra could be collected during the kinetic run, yielding direct information on the changes of the spectrum at each wavelength as a function of the protein contact time with the adsorbent surface.

In order to illustrate the importance of discrete sampling, Fig. 3 presents the emission intensity change at 350 nm as a function of time for continuous sampling (curve A) and for discrete sampling (curve B). In both cases the same amount of protein was injected. An obvious decrease in the signal with continuous sampling was observed, as a consequence of photodecomposition. This effect was clearly more important at longer sampling times than at shorter times. Thus, in the first minutes both curves had the same shape, and it was possible to assume that the effect of continuous radiation would not significantly influence kinetic measurements during this time period[18].

The second potential source of interference in the measurement of surface fluorescence intensity was Rayleigh-Tyndall scattering by the 5-μm silica particles and the protein itself and also Raman scattering mainly caused by the solvent. Fortunately, the emission of light by the tryptophan fluorophore was at a wavelength 30–50 nm longer than the excitation light (295 nm) and fluorescence could readily be separated from the scattered Rayleigh-Tyndall light[14]. In addition, 50 μg α-LACT adsorbed on the 25 mg silica surface yielded a relatively high optical density and, consequently, a relatively intense fluorescence. The excitation light was adsorbed by the protein on the surface, thus enabling light absorption to compete effectively with Raman scattering, since the latter is a weak phenomenon that is important only at high sensitivities[14]. Furthermore, a blank spectrum was obtained prior to each run and was electronically substracted from the measured spectrum. Thus, any possible effect of scattering was minimal.

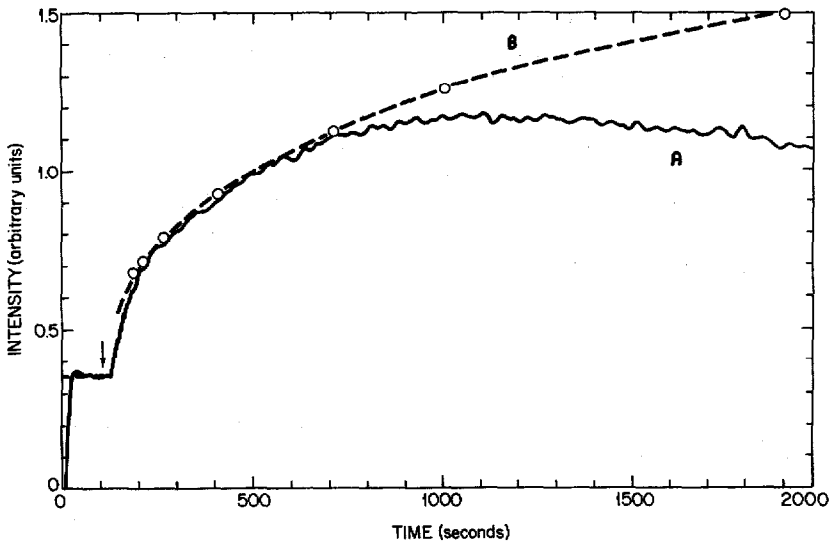

Fig. 3. The effect of photodecomposition of adsorbed α-LACT on fluorescence signal. Change of fluorescence intensity: (A) followed by continuous sampling; (B) followed by measuring discrete data points. Conditions: flow cell column packed with C1-ether phase particles; incubation solvent: 3 *M* ammonium sulfate, 0.5 *M* ammonium acetate, pH 6.3; 4°C; excitation wavelength = 295 nm; emission wavelength = 350 nm.

Solution and surface fluorescence spectra of α-LACT

Since in this work the fluorescence spectrum of α-LACT was measured in the adsorbed state, it was useful to compare the spectra of the protein on the surface with that measured in solution. Although the different states of the protein in solution could not be related directly to the species adsorbed to the surface, the change of fluorescence (*i.e.* the change of the emission maximum and quantum yield) would indicate the general level of change in the environment of the hydrophobic tryptophan residues with conformational alteration of the protein.

The solution emission maximum of α-LACT was 328 nm at 4°C in both mobile phase B (0.5 *M* ammonium acetate) and in 1 *M* ammonium sulfate plus 0.5 *M* ammonium acetate (pH 6.3). Under these conditions, the four hydrophobic tryptophans of bovine α-LACT were buried in the interior of the protein, protected from exposure to the aqueous environment[30]. A similar solution emission maximum (328 nm) was reported for the Ca^{2+} form or with other mono- and divalent protein-bound cations[20,31]. An emission maximum at roughly 330 nm thus represented the folded form of the protein. On the other hand, it was observed that thermal, acid and urea denaturation caused 15-, 15- and 20-nm red shifts, respectively, in fluorescence emission spectra of the protein. In these cases, one or more Trp units of α-LACT became exposed to the aqueous environment. The acid and temperature denatured states have been considered to be structurally very similar intermediate forms (molten globule state) and the urea denatured state to be an unfolded form of the protein[23].

The protein sample was next injected into the packed fluorescence cell and the spectrum followed as already described. Fig. 4A shows fluorescence spectra as a function of time of α-LACT adsorbed on the C1-ether phase at 4°C, with mobile phase A as the incubation solvent (3 *M* ammonium sulfate + 0.5 *M* ammonium acetate, pH 6.3). Two major features of these spectra are (1) the general increase in emission intensity with contact time and (2) the 17-nm red shift in the position of the maximum (from 330 nm in the first minute of surface contact to 347 nm after 1200 min).

The behavior of α-LACT adsorbed on the C2-ether phase is shown in Fig. 4B. It can be seen that there was a pronounced and more rapid red shift in the emission spectrum of the protein upon adsorption, with λ_{max} shifting from 331 nm to 352 nm. The fluorescence intensity also increased with the protein contact with the surface. The behavior on the two weakly hydrophobic surfaces was similar to that observed in the unfolding of α-LACT in solution[29], strongly suggesting protein conformational change on the surface.

Kinetic analysis

The rate of change of α-LACT adsorbed on the C1-ether phase was measured by the increase in fluorescence intensity at a given wavelength (350 nm) as a function of incubation time (see Fig. 5). Based on previous chromatographic results[18,27,32,33], as well as Fig. 2A and B, an attempt was initially made to fit data to a first order rate process, but the correlation was poor ($r = 0.86$). The data of Fig. 5 suggested biphasic kinetics[34,35] which can be described by a function of the form:

$$I(t) = I_\infty - (I_1^* e^{-\lambda_1 t} + I_2^* e^{-\lambda_2 t}) \quad (1)$$

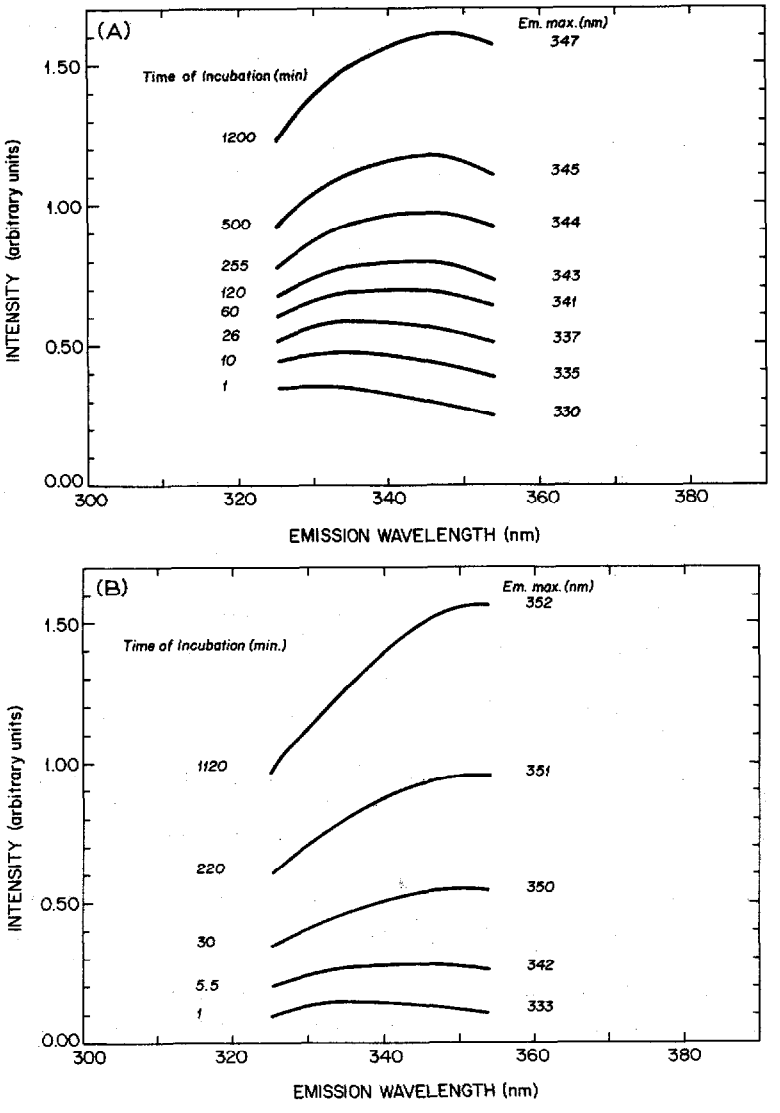

Fig. 4. Fluorescence emission spectra of α-LACT adsorbed on the (A) C1-ether phase and (B) C2-ether phase as a function of incubation time (see Fig. 3 for other conditions).

where I_1^* and I_2^* are constants (kinetic amplitudes; see below), I_∞ is the fluorescence intensity at infinite time, λ_1 and λ_2 are the macroscopic rate constants for the two steps, and t is the contact time of the protein with the surface. Fig. 5 shows the result of fitting the fluorescence intensity change as a function of contact time to eqn. 1, using a SIMPLEX-non-linear program[36]. There is an obvious excellent fit of the data.

Table I presents the values for the parameters in eqn. 1, obtained from fitting the data from three identical independent runs of the same protein solution (10-μl injection, 5 mg/ml) on the C1-ether phase. A good precision in the kinetic results was

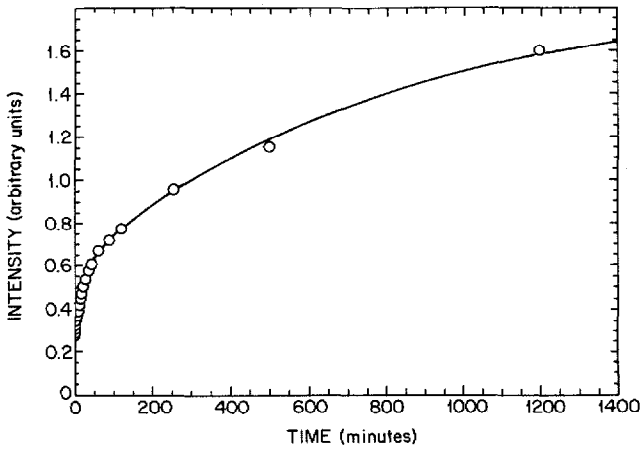

Fig. 5. Fluorescence intensity of α-LACT adsorbed on the C1-ether phase as a function of time. Fitting the fluorescence intensity data to a biphasic kinetic equation. Conditions as in Fig. 3.

obtained with the relative C.V. values for the macroscopic rate constants, λ_1 and λ_2, less than 10%. Table I also presents the value of fluorescence intensity calculated at zero time, $I(0)$; this value coincided with the value obtained by graphical extrapolation of emission intensity to zero time with a relative deviation of less than 2%. The agreement between the extrapolated and the calculated values of $I(0)$ lends further credence to the biphasic kinetic model.

The absolute value of the amplitudes, I_i^*, varied from run to run, depending on exprimental conditions. Small variations in the position of the spectrofluorometric cell, for example, produced changes in the absolute emission, but the ratio I_1^*/I_2^* was expected to be constant[34,37]. Table I shows that this ratio was indead constant.

The same analysis for the biphasic kinetic model was performed for the C2-ether phase using eqn. 1, and the results are shown in Table II. There was some similarity to the results on the C1-ether phase (Table I); however, two important differences were found: (1) the ratio between the kinetic amplitudes, I_1^*/I_2^*, was almost four times larger: 1.19 (C2-ether) *vs.* 0.26 (C1-ether); and (2) the macroscopic rate constants were also

TABLE I

KINETIC PARAMETERS FOR BIPHASIC KINETICS FOR THE UNFOLDING OF α-LACT

C1-ether phase, 4°C, from eqn. 1[a].

Run No.	I_∞	I_1^*	I_2^*	$I(0)^b$	I_1^*/I_2^*	λ_1 (min^{-1}) ($\times 10^2$)	λ_2 (min^{-1}) ($\times 10^3$)
1	1.75	0.38	1.21	0.32	0.31	5.9	1.6
2	1.85	0.33	1.26	0.26	0.26	5.4	1.3
3	1.72	0.30	1.18	0.24	0.25	6.6	1.5
				Mean ± S.D.		6.0 ± 0.5	1.5 ± 0.1

[a] Conditions as in Fig. 3; fluorescence emission intensity followed at 350 nm.
[b] Eqn. 1 evaluated at $t = 0$.

TABLE II

KINETIC PARAMETERS FOR BIPHASIC KINETICS FOR THE UNFOLDING OF α-LACT

C2-ether phase, 4°C, from eqn. 1[a].

Run No.	I_∞	I_1^*	I_2^*	$I(0)^b$	I_1^*/I_2^*	λ_1 (min^{-1}) ($\times 10^2$)	λ_2 (min^{-1}) ($\times 10^3$)
1	1.70	0.55	0.40	0.26	1.22	7.8	6.9
2	1.78	0.56	0.44	0.26	1.27	7.7	6.5
3	1.89	0.52	0.48	0.25	1.08	8.5	6.9
				Mean ± S.D.		8.0 ± 0.3	6.7 ± 0.2

[a] Conditions as in Fig. 3; fluorescence emission intensity followed at 350 nm.
[b] Eqn. 1 evaluated at $t = 0$.

larger, *e.g.* $\lambda_2 = 6.7 \cdot 10^{-3}$ min^{-1} (C2-ether) *vs.* $1.5 \cdot 10^{-3}$ min^{-1} (C1-ether). A more rapid structural change on the C2-ether phase was expected, given the greater hydrophobicity of this phase. The results of Tables I and II thus suggested that the molecular kinetic events were related to the direct interaction between the protein and the adsorbent surface.

Since in this study the protein was expected to be concentrated at the top of the cell-column, the possibility existed of time dependent surface protein–protein interaction leading to the rate behavior in Fig. 5. If this were the case, the macroscopic rate constant in eqn. 1 would be concentration dependent, and, at the same time, the data would be best represented by second order kinetics. To demonstrate that protein–protein interaction did not affect the kinetics at the protein concentration level used in this work, the concentration of the injected sample was varied and the rate constants measured on the C2-ether phase. An increase of four-fold in the concentration of a 10-μl injection volume (2–8 mg/ml) did not significantly change the value of the macroscopic rate constants (C.V. < 10%) and only slightly affected the ratio of the amplitudes (C.V. < 15%). In addition, the reciprocal plot of intensity *vs.* time was not linear ($r^2 = 0.25$) which indicated that second order kinetics (expected for 1:1 protein interaction) did not hold. The experimental parameters of eqn. 1 could thus be considered to be independent of sample concentration in this concentration range. Obviously, in higher concentration regions, the kinetics (and emission maxima) could be sample concentration dependent.

It is also important to note that the observed rate constants were independent of the linear flow-rate of the mobile phase from 0 to 0.5 ml/min (higher flow-rates were not possible because of the fragility of the packed flow cell). This result suggested that the protein adsorbed to the support mainly within the pores where no flow occurred.

The classical criterion for the existence of a unimolecular reaction (*i.e.*, one chemical entity continuously changing) is the independence of the kinetic rate constants on the wavelength selected to follow the reaction[38]. Therefore, in order to explore further the biphasic process, the change in emission intensity with time was measured during the same run at three different wavelengths: 334, 342 and 350 nm (correcting for the slight difference in time between wavelength sampling). Within experimental error, the same value of the macroscopic rate constants and the same ratio of the amplitudes (< 10%) were obtained at each wavelength. As a consequence,

the reaction kinetics were independent of the wavelength selected and corresponded to a unimolecular process.

At least three states were therefore assumed to be involved in the process, the initial folded state (F), the final unfolded state (U), and a kinetic intermediate state (X). U is not meant to imply that unfolding ceases at this point since with further contact of the protein with the surface increased structural changes could occur. We will discuss later the extent of unfolding of the kinetic intermediate. We next examine the kinetic mechanism of protein change on the surface.

Kinetic model

A general mechanism that has been used to describe biphasic kinetics is[39]

$$\mathrm{F} \underset{k_2}{\overset{k_1}{\rightleftarrows}} \mathrm{X} \underset{k_4}{\overset{k_3}{\rightleftarrows}} \mathrm{U} \tag{2}$$

where k_i is the microscopic rate constant of process i. The general solution of this kinetic model in terms of the measured parameters of eqn. 1 is

$$I_0^* = k_2k_4/\lambda_1\lambda_2 \tag{3}$$

$$I_1^* = k_1(\lambda_1 - k_3 - k_4)/\lambda_1(\lambda_1 - \lambda_2) \tag{4}$$

$$I_2^* = k_1(k_3 + k_4 - \lambda_2)/\lambda_2(\lambda_1 - \lambda_2) \tag{5}$$

where I_i^*, as noted previously, is the kinetic amplitude associated with phase i, and the other terms have been defined before. I_0^* corresponds to the preexponential term obtained from the solution of the differential equation that describes the system, *i.e.* the term $e^{-\lambda_0 t}$, where $\lambda_0 = 0$ is one of the roots of the equation:

$$I = I_\infty - \sum_0^2 I_i \exp(-\lambda_i t) \tag{6}$$

Eqns. 3–5 can be used to obtain the microscopic rate constants of the general kinetic mechanism described in eqn. 2. Combination of eqns. 4 and 5 yields the value of k_1 for conversion of F to X:

$$k_1 = (\lambda_1 I_1^* + \lambda_2 I_2^*) \tag{7}$$

Since the experimental data sets are correctly described by a two kinetic amplitude function, eqn. 1, it can be deduced that I_0^* must be equal to zero in the time range of the experiments. Therefore, the right-hand side of eqn. 3 must be equal to zero, and either k_2 or k_4 or both rate constants must equal zero, since for two consecutive reactions a parabolic function of I *vs.* t would result[39]. If k_2 were equal to zero, a sigmoidal curve of I *vs.* t would be observed[40]. Since neither parabolic nor sigmoidal behavior was found, it can be concluded that $k_4 = 0$. The irreversible nature of the final step is not surprising, given the surface kinetic models suggested by others[41–43]. Therefore, the final kinetic model can be written as:

$$F \underset{k_2}{\overset{k_1}{\rightleftarrows}} X \xrightarrow{k_3} U \tag{8}$$

Using the value for k_1 in eqn. 7, eqns. 4 and 5 can be combined to yield a solution for k_3:

$$k_3 = \lambda_1\lambda_2(I_1^* + I_2^*)/(\lambda_1 I_1^* + \lambda_2 I_2^*) \tag{9}$$

In order to find k_2, the following relationship between the macroscopic and microscopic rate constants can be used[37]:

$$\lambda_1 + \lambda_2 = k_1 + k_2 + k_3 \tag{10}$$

With appropriate experimental values in eqns. 7, 9 and 10, the microscopic rate constants for both the C1-ether and C2-ether phases were determined (see Table III). The values correspond to relatively slow processes: the time constants for the formation of the intermediate ($\tau_1^{-1} = k_1 + k_2$) are 18 and 13 min for the C1-ether and the C2-ether phases, respectively. The half-life of the second process (formation of U) at 4°C is 111 min for the C1-ether phase and 58 min for the C2-ether phase.

The principle of microscopic reversibility permits the calculation of the equilibrium constant, K_e, for the process F $\rightleftarrows$ X using the microscopic rate constants k_1 and k_2. From Table III, a value of $K_e = 0.66$ was obtained on the C1-ether phase, whereas on the C2-ether phase, $K_e = 1.55$. These values indicate that at 4°C the formation of the kinetic intermediate is thermodynamically more favorable on the C2-ether phase (with $\Delta G < 0$) than on the C1-ether phase.

From the microscopic rate constants it is possible to obtain the fraction of each species as a function of time, $Y_i(t)$, using the integrated rate law for each component[39]. The results of this calculation for both adsorbents are shown in Fig. 6. For the C1-ether phase the maximum fraction of kinetic intermediate, X, which was reached after 40 min, represented 20% of the total amount of protein. For the C2-ether phase the maximum was reached after 33 min, representing 46% of the total amount of protein. Not surprisingly, there was a greater accumulation of the kinetic intermediate on the C2-ether phase.

Calculation of normalized emission fluorescence spectra

The above kinetic model can be used to obtain the normalized emission spectra of each of the three species. Such an approach can provide information on the spectroscopic nature of the various states of the protein on the surface.

The fluorescence intensity at wavelength λ and at time t, $I_\lambda(t)$, is the sum of the individual intensities of the species present on the surface:

$$I_\lambda(t) = \Phi_1 Y_F(t) + \Phi_2 Y_X(t) + \Phi_3 Y_U(t) \tag{11}$$

where Φ_i is the product of quantum yield, optical pathlength of the cell, and extinction coefficient of species i at wavelength λ, and $Y_i(t)$ is the fraction of species i at time t. The data of the spectra of Fig. 4A and B and the calculated individual fractions of each species (see Fig. 6) at three specific surface contact times were used in eqn. 11 to yield

TABLE III

MICROSCOPIC RATE CONSTANTS AT 4°C FOR UNFOLDING OF α-LACT ON THE C1-ETHER PHASE AND THE C2-ETHER PHASE

Conditions: see Fig. 3.

Microscopic rate constant	*C1-ether phase* (min^{-1})	*C2-ether phase* (min^{-1})
k_1	$2.17 \cdot 10^{-2}$	$4.57 \cdot 10^{-2}$
k_2	$3.31 \cdot 10^{-2}$	$2.94 \cdot 10^{-2}$
k_3	$6.25 \cdot 10^{-3}$	$1.19 \cdot 10^{-2}$
k_4	0	0

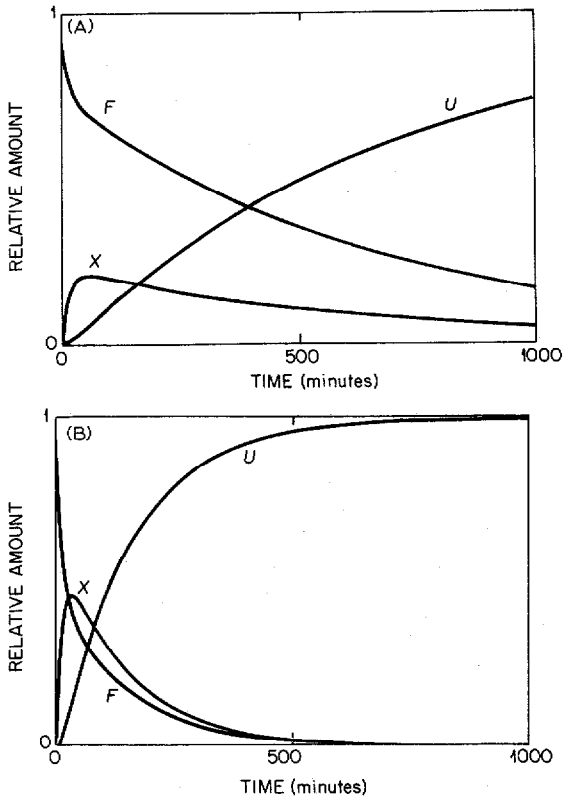

Fig. 6. Relative amounts of F (folded), X (kinetic intermediate) and U (unfolded) states as a function of time for α-LACT, adsorbed at 4°C on (A) C1-ether phase and (B) C2-ether phase. The model is based on biphasic kinetics. Conditions as in Fig. 3.

sets of Φ_i for F, X and U at each wavelength. These values were then plotted as a function of wavelength, yielding individual normalized emission spectra. The results are shown in Fig. 7 for α-LACT adsorbed on the C1-ether and the C2-ether phases.

Consider first the calculated normalized individual spectra on the C1-ether phase. The maximum in the spectrum of the folded species F was 331 nm; this value closely agreed with that observed in Fig. 4 after the first minute of contact with the surface. The maximum of the spectrum of the unfolded species, U, was 348 nm, also in agreement with the value of 347 nm obtained in Fig. 4 after 1200 min. The position of the maximum in the spectrum of X at 345 nm suggested that this state was more spectroscopically similar to the unfolded species than to the folded state, but, as will shortly be seen, the spectrum does not necessarily reflect the binding strength of the species to the surface. Note also the normalized intensity of this species was only half that of U.

The wavelength maxima of the three spectra on the C2-ether phase (Fig. 7B) showed a red shift for each species relative to that observed for the corresponding species on the C1-ether phase: for the folded form F the shift was from 331 nm to 333 nm, for the kinetic intermediate, X, from 345 nm to 350 nm, and the unfolded, U, from 348 nm to 352 nm. There was again agreement between the calculated and

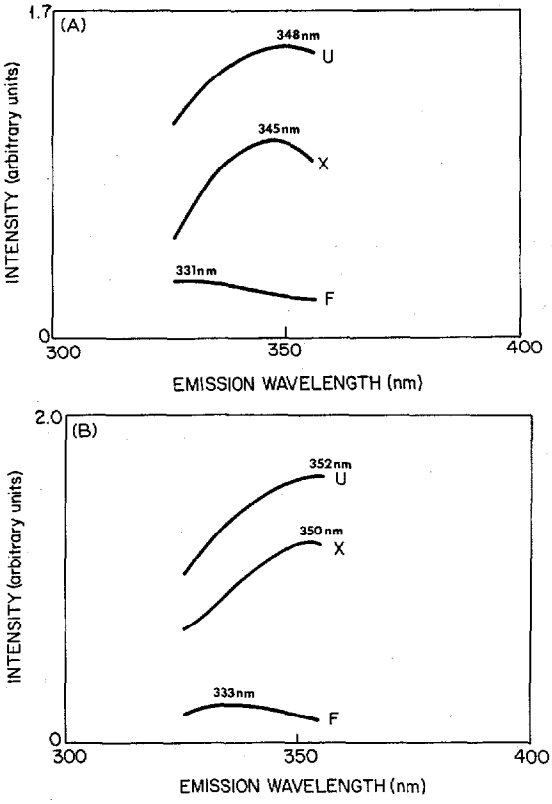

Fig. 7. Calculated spectra for the F, X and U forms on the (A) C1-ether phase and (B) C2-ether phase from eqn. 11.

experimental wavelength maxima for the unfolded and folded states. Morevover, the normalized intensity of X was again approximately halfway between F and U.

Activation parameters

Surface fluorescence emission spectra as a function of protein contact time were obtained at several temperatures: 4, 10, 20 and 30°C for the C1-ether phase, and 4, 8 and 10°C for the C2-ether phase. (Studies over 10°C were not possible on the C2-ether phase because the kinetic process was too fast to measure.) In each run the same amount of protein was injected, and the same column was used throughout the study. At least three runs were performed at each temperature.

Assuming that the system is well described by the proposed mechanism of eqn. 8 and following the absolute rate theory, which has been applied on surfaces[41] as well as solution unfolding–refolding of proteins[42], it was possible to obtain information on the thermodynamic parameters of activation of each step in the kinetic mechanism.

The relationship between activation enthalpy, $\Delta H^{\#}$, and activation energy, E_a, for a unimolecular reaction is:

$$\Delta H^{\#} = E_a - RT \tag{12}$$

E_a is related to the specific rate constant k by the Arrhenius equation:

$$k = A \exp(-E_a/RT) \tag{13}$$

where the preexponential factor A is related to the activation entropy, $\Delta S^{\#}$:

$$A = 2.3\ (\kappa T/h)\ \exp\ (\Delta S^{\#}) \tag{14}$$

where h is the Planck constant and κ is the Boltzmann constant. Using eqns. 12–14, the values of each activation parameter and the subsequent thermodynamic parameters were calculated for 4°C as shown in Table IV. Fig. 8 displays the data of the tables in order to discern more clearly differences between the two phases.

It can be first noted that the activation energy to form the kinetic intermediate ($E_{a\,(F\rightarrow X)}$) on the C1-ether phase was greater than on the C2-ether phase (103 *vs.* 46 kJ/mol). This result was expected, *i.e.* the formation of the kinetic intermediate proceeded faster on the more hydrophobic phase.

On the C1-ether phase (Fig. 8A), the formation of X involved an endothermic process ($\Delta H_{F\rightleftarrows X} = 24$ kJ/mol) with a favorable entropy ($\Delta S_{F\rightleftarrows X} = 85$ J/K mol). On the other hand, on the C2-ether phase the opposite occurred with an exothermic conversion of F to X ($\Delta H_{F\rightleftarrows X} = -50$ kJ/mol) and a large negative or unfavorable entropy ($\Delta S_{F\rightleftarrows X} = -177$ J/K mol). Evidently, on the less hydrophobic phase, the protein unfolded to expose tryptophan residues (based on Fig. 7A) but the interaction of X with the support was weaker than on the C2-ether phase. The large favorable increase in entropy on the C1-ether phase may be due in part to release of water molecules as a part of the hydrophobic interaction and to the conformational change. On the C2-ether phase, there was not only a conformational change in the formation of X (see Fig. 7B) but this species could then bind relatively stronger to the hydrophobic surface. The loss in entropy in this case may in part be due to a rigidity in the molecule caused by the binding.

TABLE IV

MICROSCOPIC ACTIVATION PARAMETERS FOR THE C1 AND C2-ETHER PHASES AT 4°C

Conditions: see Fig. 3.

Phase	*Reaction*	E_a *(kJ/mol)*	$\Delta H^{\#}$ *(kJ/mol)*	$\Delta S^{\#}$ *(J/K mol)*	$\Delta G^{\#}$ *(kJ/mol)*
C1-ether	F → X	103 ± 8	101 ± 8	100 ± 20	73 ± 2
	X → F	79 ± 5	77 ± 5	15 ± 4	73 ± 2
	X → U	76 ± 5	74 ± 5	3 ± 2	73 ± 2
C2-ether	F → X	46 ± 10	44 ± 3	−107 ± 8	71 ± 2
	X → F	96 ± 5	94 ± 5	70 ± 7	76 ± 2
	X → U	118 ± 5	116 ± 5	143 ± 8	78 ± 3

On the C1-ether phase there was equal favorability for the formation of F or U from X, as E_a was roughly equivalent for both processes. On the other hand, due to the binding of X to the C2-ether phase there was a significant activation energy to form U or to reconvert back to F on this phase. Furthermore, on the C1-ether phase, $E_{a\,(F\to X)}$ was much greater than $E_{a\,(X\to U)}$, whereas the opposite was true on the C2-ether phase. For this reason, as well as the larger value of $E_{a\,(X\to U)}$ and lower value of $E_{a\,(F\to X)}$ on the more hydrophobic phase, X accumulated to a greater extent and also at shorter protein surface contact times on the C2-ether phase (see Fig. 6).

It is interesting to note in Table IV that the activation free energy ($\Delta G^{\#} = \Delta H^{\#} - T\Delta S^{\#}$) of the processes F → X and the reverse X → F on the C1-ether phase were the same (73 kJ/mol), indicating that the adsorption free energies of F and X were similar. On the other hand, on the C2-ether phase, $\Delta G^{\#}$ for the process F → X was 71 kJ/mol whereas it was 76 kJ/mol for the reverse process X → F. The 5-kJ/mol

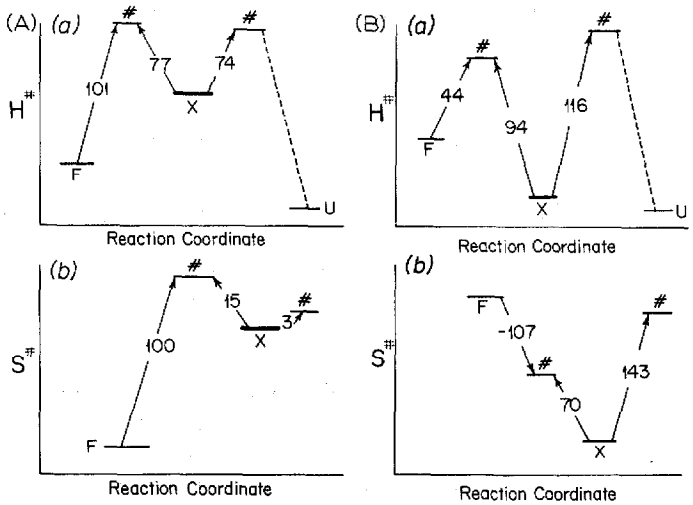

Fig. 8. Enthalpy and entropy of activation diagrams for the process of unfolding of α-LACT on the (A) C1-ether phase and (B) C2-ether phase. Other conditions as in Fig. 3. (a) Enthalpy diagrams, (b) entropy diagrams.

difference in activation free energies further indicates that X binds to the C2-ether phase more strongly.

In summary, while both phases followed the same biphasic kinetic rate law, there were significant differences in the detailed mechanism of unfolding. The activation parameters, determined from the temparature dependence of the microscopic rate constants, were very important in elucidating a more detailed picture of the process.

Solution refolding

Previously, using on-line second derivative UV spectroscopy, it was concluded that at least two species were present in the broad second chromatographic peak of α-LACT eluted from the C2-ether column[27]. It was suggested that the surface unfolded protein represented by the second peak could refold in solution upon desorption from the surface.

In this work we measured the solution rate of fluorescence change of each eluted species. The mobile phase flow was stopped when the first eluted and subsequently the second eluted peak reached the empty flow cell II (see Fig. 1). The solution fluorescence emission maxima of the first chromatographic peak in flow cell II on both the C1-ether and C2-ether phases, as expected, were found to be 328 nm, and no change of the intensity with time was observed.

At 4°C the elution salt concentration of the second peak on the C1-ether phase was 0.70 *M* ammonium sulfate (pH 6.3). A shift in emission maximum from approximately 342 nm to 328 nm was observed in the second cell, indicating a solution refolding process[25]. In addition, the natural logarithm of the corrected fluorescence intensity change at 350 nm *vs.* time was linear ($r^2 = 0.9952$) with a first order rate constant for refolding of $6.9 \cdot 10^{-1}$ min^{-1} ($t_{1/2} = 1.0$ min). A similar emission maximum change of the second peak occurred on the C2-ether phase. The rate of refolding was measured to be $7.4 \cdot 10^{-1}$ min^{-1} ($t_{1/2} = 0.9$ min; $r^2 = 0.9873$). It is interesting to note that the rate constants for the two phases were not statistically different at the 95% confidence level from the value of $7.8 \cdot 10^{-1}$ min^{-1} ($t_{1/2} = 0.9$ min) at 4°C (pH 7), reported for the slow step of the biphasic refolding process of α-LACT in solution[25]. This result is expected since the previous cited study showed that the intermediate state accumulated instantaneously during solution refolding, irrespective of the original extent of unfolding of the protein[25]. In addition, because of this finding, it is not possible to conclude whether the extent of unfolding of U on the two phases was the same, even though the rate of solution refolding was similar.

Finally, the broad second chromatographic peak on the C2-ether phase (see Fig. 2B), can be attributed to isocratic elution and not to refolding in the mobile phase during migration through the column[43]. The roughly 1 min half-life for refolding of α-LACT is significantly longer than the 0.1 min necessary to travel in the mobile phase through the microcolumn. On the other hand, the half-life is comparable to the unretained species time of the previously used 10-cm column, and it is quite possible that both isocratic elution and slow refolding in the mobile phase contributed to the broadened peak in that study[27]. In agreement with this conclusion, it was found that on-line UV spectroscopic characteristics of the band were different on the front and the rear sides[27].

Model for surface unfolding of α-LACT

Based on the results of this study, the kinetic model of α-LACT unfolding on the two weakly hydrophobic phases is illustrated in Fig. 9A and B. On both surfaces there was observed to be a kinetic intermediate, followed by a more unfolded state, leading to biphasic kinetics on each support. Based on the activation free energies, X on the C1-ether phase adsorbed with approximately the same strength as the folded form; however, X interacted with the surface with 5 kJ/mol greater strength than the folded form on the C2-ether phase. This latter difference was most likely a result of the greater hydrophobicity of the C2-ether phase. The increased accumulation of X on the C2-ether phase (see Fig. 6) was in part a result of the greater barrier for surface refolding of this more tightly bound species.

Fluorescence spectroscopic results suggest that the kinetic intermediates on both phases have significant unfolding, according to the roughly 17-nm red shift in the tryptophan emission maximum. Based on the data available, however, it is not possible to determine further the properties of X. The kinetic intermediate may be an unfolded form in which the process of X → U is a proline *cis–trans* isomerization[44]. It should also be pointed out that reorientation of X on the surface to form U cannot be ruled out. However, studies of α-LACT reveal intermediates in the unfolding and refolding pathways in solution[23–25], and the formation of an intermediate on the surface would not be surprising. More study of the surface structure of X and U (as well as F) would be of value in a further elucidation of the surface processes.

Finally, Fig. 9A and B can be compared to the previous kinetic model for protein adsorption put forward by Lundstrom *et al.*[45] and discussed in detail by Andrade[46,47]. In that model, it was assumed that F converted on the surface into a series of unfolded states U_1, U_2, etc., each step being an irreversible process. In our study, irreversibility was also observed; however a reversible kinetic intermediate was part of the unfolding pathway. In addition, in agreement with the above cited model, we observed refolding of U to F in solution.

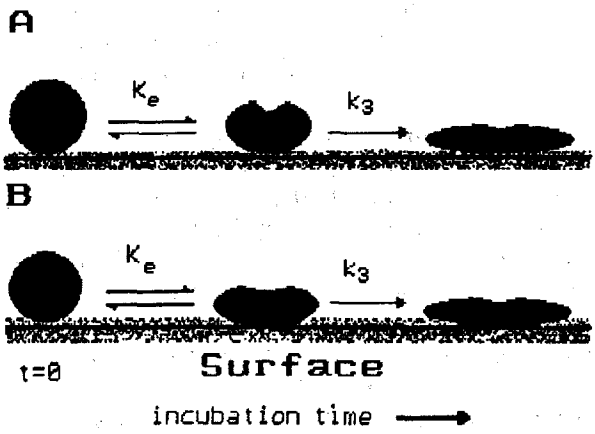

Fig. 9. Kinetic model of unfolding of α-LACT on (A) C1-ether phase and (B) C2-ether phase (see the text for details).

CONCLUSIONS

The kinetics of the slow unfolding process of α-LACT on two different hydrophobic surfaces have been examined using hydrophobic interaction chromatography and intrinsic fluorescence spectroscopy. The chromatographically determined rates of unfolding of small globular adsorbed proteins have generally been described by a first order rate process without any reference to microscopic events[18,29,33]. The surface intrinsic fluorescence behavior of α-LACT permitted a more detailed picture of the kinetic process where biphasic kinetics was observed. The good fit of a two-state model based on first order kinetics in the chromatographic procedure may simply be due to the poor time resolution of the measurements.

The half-lives of species obtained from the fluorescence measurements were much longer than those normally observed for solution unfolding processes, the latter of which are in the order of milliseconds to seconds[40]. One must remember, however, that low temperature was used and that the incubation solvent was highly antichaotropic and thus stabilizing. Solution unfolding of the protein would not occur under these conditions. The surface was therefore catalyzing an unfavorable process under these conditions.

The results demonstrate the potential of combining chromatography with intrinsic fluorescence of proteins adsorbed on surfaces. The chromatographic results focus on the binding strengths of species to a surface as well as the thermodynamic differences of various conformational states. On the other hand, fluorescence measurements provide direct insight into surface processes since studies are conducted while the protein is in contact with the adsorbent surface. Both kinetic as well as surface structural details can be discerned from such measurements.

The precision of the kinetic data (C.V. $< 10\%$) is worth noting. With such precise kinetic rate constants, small and subtle differences in species can potentially be observed. This suggests that the kinetics of surface conformational change of peptide/protein species may potentially be used as a sensitive determination of variants, as already developed for solution studies[48]. In addition, surface fluorescence measurements may be useful for adsorbent characterization. As seen in this paper, the hydrophobicity of the support altered not only the rate constants, but also the activation energies. Indeed, the combination of chromatography and fluorescence may prove to be a very powerful analytical tool for solute and adsorbent characterization.

Using the combination of surface fluorescence and chromatography, a variety of important parameters in chromatographic operation can be explored in detail. For example, the role of protein surface concentration on the extent and the rate of surface unfolding can be studied. For the adsorbent, the possible differences between the surface within a pore and that on the external portion of the particle may be examined. In addition, dynamic fluorescence measurements such as lifetime and anisotropy decay may provide further insight into surface induced unfolding processes[13]. Moreover, the direct study of surface processes opens up the possibility to design surfaces for specific needs, *e.g.* biomaterials, catalysts and separation media.

Finally, as noted in the introduction, chromatography of biopolymers often involves (knowingly or unknowingly) conformational manipulation to achieve selective separation. Surface fluorescence coupled with chromatographic elution

provides a means of probing the structural, thermodynamic and kinetic processes involved in adsorption and desorption. Through these and other studies, rational optimization of chromatographic conditions for biopolymer separation may be achieved. It is through a detailed understanding of surface processes that advances can be made in the manipulation of proteins on surfaces.

SYMBOLS

A	preexponential factor of eqn. 13
E_a	activation energy of the individual microscopic kinetic steps
F	folded form of the protein
h	Planck constant
I_i^*	amplitude of the kinetic phase i
$I(t)$	fluorescence intensity at time t
$I_\lambda(t)$	emission intensity at wavelength λ and time t
I_∞	fluorescence intensity at infinite time
K_e	equilibrium constant of the process F $\rightleftarrows$ X
k_i	microscopic rate constant of the kinetic step i
R	gas constant
T	temperature
t	contact time of protein with surface
$t_{1/2}$	kinetic half-life
U	unfolded form of the protein
X	intermediate form of the protein
$Y_i(t)$	fraction of species i during the kinetic process F $\rightleftarrows$ X $\rightarrow$ U at time t
$\Delta G^\#$	activation free energy change
$\Delta H^\#$	activation enthalpy change
$\Delta S^\#$	activation entropy change
Φ_i	product of the optical pathlength, quantum yield and extinction coefficient of species i
κ	Boltzmann constant
λ_i	macroscopic rate constant of the kinetic phase i
τ	time constant of the reversible kinetic process F $\rightleftarrows$ X

ACKNOWLEDGEMENTS

The authors gratefully acknowledge NIH GM15847 for support of this work. R.B. acknowledges the support of a scholarship from CONICIT-UCR and the Supreme Court of Costa Rica.

Contribution No. 389 from the Barnett Institute.

REFERENCES

1 T. A. Horbett and J. L. Brash, in J. L. Brash and T. A. Horbett (Editors), *Proteins at Interfaces: Physicochemical Aspects and Biochemical Studies*, American Chemical Society, Washington, DC, 1987, p. 1.
2 F. E. Regnier, *Science (Washington, D.C.)*, 238 (1987) 319.
3 J. D. Andrade and V. Hlady, in J. D. Andrade (Editor), *Advances in Polymer Science*, Vol. 79, Springer, New York, 1986, p. 1.

4 K. Benedek, S. Dong and B. L. Karger, *J. Chromatogr.*, 317 (1984) 227.
5 S. Shaltiel, *Methods Enzymol.*, 104 (1984) 69.
6 W. R. Melander, H.-J. Lin, J. Jacobson and Cs. Horváth, *J. Phys. Chem.*, 88 (1984) 4527.
7 M. E. Soderquist and A. G. Walton, *J. Colloid Interface Sci.*, 75 (1980) 389.
8 B. Furie, R. A. Blanchard, D. J. Robinson, M. M. Tai and B. C. Furie, *Methods Enzymol.*, 125 (1982) 60.
9 B. M. Morrisey, L. E. Smith, R. R. Stromberg and C. A. Fenstermaker, *J. Colloid Interface Sci.*, 56 (1976) 557.
10 R. M. Gendreau, S. Winters, R. I. Leininger, D. Fink and C. R. Hassler, *Appl. Spectrosc.*, 35 (1981) 353.
11 A. Aurengo, M. Masson and E. Dupeyrat, *Appl. Opt.*, 22 (1982) 602.
12 G. R. McMillin and A. G. Walton, *J. Colloid Interface Sci.*, 48 (1974) 345.
13 J. R. Lakowicz, *Principles of Fluorescence Spectroscopy*, Plenum, New York, 1983, p. 342.
14 B. Gabel, Z. Z. Steinberg and E. Katchalski, *Biochemistry*, 10 (1971) 4661.
15 R. W. Watkins and C. R. Robertson, *J. Biomed. Mater. Res.*, 11 (1977) 915.
16 S. A. Darst, C. R. Robertson and J. A. Berzofsky, *J. Colloid Interface Sci.*, 111 (1986) 466.
17 C. H. Lochmuller and S. S. Saavedra, *Langmuir*, 3 (1987) 433.
18 X. M. Lu, A. Figueroa and B. L. Karger, *J. Am. Chem. Soc.*, 110 (1988) 1978.
19 B. L. Karger and R. Blanco, in T. W. Hutchens (Editor), *Protein, Structure, Folding and Design*, Alan R. Liss, New York, 1989, p. 141.
20 D. I. Stuart, K. R. Acharya, N. P. C. Walker, S. G. Smith, M. Lewis and D. C. Phillips, *Nature (London)*, 324 (1986) 84.
21 Y. Hirioka, T. Segawa, K. Kuwajima, S. Sugai and N. Murai, *Biochem. Biophys. Res. Commun.*, 95 (1980) 1098.
22 W. Pfeil, in M. M. Jones (Editor), *Biochemical Thermodynamics*, Elsevier, Amsterdam, 1988, p. 53.
23 J. Baum, C. M. Dobson, P. A. Evans and C. Hanley, *Biochemistry*, 28 (1989) 7.
24 M. Ikeguchi, K. Kuwajima, M. Mitani and S. Sugai, *Biochemistry*, 25 (1986) 6965.
25 Y. Harushima, K. Kuwajima and S. Sugai, *Biopolymers*, 27 (1988) 629.
26 S. L. Wu, K. Benedek and B. L. Karger, *J. Chromatogr.*, 359 (1986) 3.
27 S. L. Wu, A. Figueroa and B. L. Karger, *J. Chromatogr.*, 371 (1986) 3.
28 N. T. Miller, B. Feibush and B. L. Karger, *J. Chromatogr.*, 316 (1985) 519.
29 A. V. Ostrovsky, L. P. Kalinichenko, V. I. Emelyanenko, A. V. Klimanov and E. A. Permyakov, *Biophys. Chem.*, 30 (1988) 105.
30 J. C. L. van Ceunebrock, J. Krebs, I. Hannsens and F. van Cauwelaert, *Biochem. Biophys. Res. Commun.*, 95 (1986) 604.
31 E. A. Permyakov, L. A. Morozova and E. A. Burnstein, *Biophys. Chem.*, 21 (1985) 21.
32 S. A. Cohen, K. Benedek, S. Dong and B. L. Karger, *Anal. Chem.*, 56 (1984) 217.
33 K. Benedek, *J. Chromatogr.*, 458 (1988) 93.
34 A. Ikai and C. Tanford, *J. Mol. Biol.*, 73 (1973) 145.
35 A. M. Labhardt and R. L. Baldwin, *J. Mol. Biol.*, 135 (1979) 231.
36 J. H. Noggler, *Physical Chemistry on a Microcomputer*, Little & Brown, Boston, MA, 1985, p. 145.
37 P. J. Hagerman, *Biopolymers*, 16 (1977) 731.
38 A. Ikai, W. W. Fish and C. J. Tanford, *J. Mol. Biol*, 73 (1973) 165.
39 J. W. Moore and R. G. Pearson (Editors), *Kinetics and Mechanism*, Wiley, New York, 1981, p. 296.
40 F. X. Schmid, *Methods Enzymol.*, 131 (1986) 70.
41 K. J. Laidler (Editor), *Chemical Kinetics*, Harper & Row, Cambridge, MA, 1987, p. 258.
42 P. J. Hagerman and R. L. Baldwin, *Biochemistry*, 15 (1975) 1462.
43 S. A. Cohen, K. Benedek, Y. Tapuhi, J. C. Ford and B. L. Karger, *Anal. Biochem.*, 144 (1985) 275.
44 P. S. Kim and R. L. Baldwin, *Ann. Rev. Biochem.*, 51 (1982) 549.
45 I. Lundstrom, B. Ivarson, U. Jonsson and H. Elwing, in W. J. Feast and H. S. Munro (Editors), *Polymer Surfaces and Interfaces*, Wiley, New York, 1987, p. 201.
46 J. D. Andrade, *Ann. N.Y. Acad. Sci.*, 516 (1987) 158.
47 J. D. Andrade, in J. D. Andrade (Editor), *Surface and Interfacial Aspects of Biomedical Polymers*, Vol. 2, Plenum, New York, 1985, p. 1.
48 D. P. Goldenberg, *Annu. Rev. Biophys. Biophys. Chem.*, 17 (1988) 481.